

Muon Cooling Channels

Eberhard Keil

Katharinenstr. 17, DE-10711 Berlin, Germany

Abstract

Parameters of muon cooling channels are discussed that achieve cooling of a muon beam from initial to final emittances in all three degrees of freedom in a given length. Published theories of ionisation cooling yield equilibrium emittances from multiple scattering and energy straggling, and partition numbers. Limits are obtained on the amplitude functions in all three degrees of freedom. Parameters of wedge-shaped absorbers and partition numbers are derived for simultaneous longitudinal and transverse cooling. Limits on length and material of absorbers, and dispersion at the wedge-shaped absorbers are obtained. Parameters are presented for the RF system, e.g. peak voltage, frequency, stable phase angle. The properties of the magnetic lattice which satisfies the conditions imposed by the longitudinal dynamics are studied. The consequences of changes in the assumed performance of the cooling channel on its parameters are discussed.

Key words: Ionisation cooling, cooling ring, cooling channel

PACS: 29.27.+w, 29.20.Mr, 34.50.-s, 34.50.B

1 Introduction

The aim of this paper is taking the reader step by step through the design of a muon cooling channel that reduces the normalised emittances from assumed initial values, typical for a muon cooling channel, to assumed final values in 6D over a distance S . Physics issues will be recapitulated as they arise during the design. The paper is intended to educate non-specialists in cooling muons by ionisation, and to contribute to their understanding of the physics in muon cooling channels, but hopefully also to give views that specialists find interesting.

Email address: e-mail Eberhard.Keil@t-online.de (Eberhard Keil).

Table 1

Possible combinations of shape and focusing in muon cooling channels

Shape	Focusing
Straight	Solenoid
Ring	Quadrupole

Tab. 1 shows four possible combinations of shape and focusing in a muon cooling channel. All of them have been proposed and studied. Straight channels were incorporated in Studies I [1] and II [2]. They have transverse cooling, no dispersion, no wedge-shaped absorbers, and longitudinal heating due to straggling. Ring coolers were invented more recently, and have dispersion at wedge-shaped absorbers, and transverse and longitudinal cooling. The example in this paper has both transverse and longitudinal cooling.

2 Analytical Theory

The design procedure outlined in this paper does not use simulation, but analytical theory that was verified by simulation, and is good enough for parameter searches and design purposes. It will be checked by the proposed experiment MICE [3]. It is implemented in *Mathematica* notebooks that make generating sets of parameters quick and, perhaps too easy. The theory averages the quantities along channel, indicated by $\langle \dots \rangle$ in the equations below. For simplicity, I replace averages by local values wherever possible. I do not advocate particular channel styles and devices. In the remainder of this Section, I assemble the theory [4,5], and introduce my notation.

Briefly, transverse ionisation cooling works as follows. The energy loss $\langle dE/ds \rangle$ in an absorber reduces the muon momenta in all three degrees of freedom, two transverse x and y , and one longitudinal s . Acceleration by an RF system compensates the loss in longitudinal momentum. Longitudinal cooling is achieved with wedge shaped absorbers, where $\langle dE/ds \rangle$ depends on the lateral orbit offset y , and by choosing $D_y \neq 0$ at the absorber such that muons with higher longitudinal momentum lose more of it in a longer absorber. Multiple scattering and straggling in the absorber counteract the cooling. When one averages the s -dependent quantities, one can write the solution of the differential equation for the normalised emittance $\varepsilon(s)$ with $\varepsilon^i = \varepsilon(s = 0)$, introducing the cooling length s_c , and the equilibrium emittance ε^{eq} , noting that ε^{eq} is asymptotically reached from above:

$$\varepsilon(s) = \varepsilon^{eq} + (\varepsilon^i - \varepsilon^{eq}) \exp(-s/s_c) \quad (1)$$

The longitudinal cooling length s_c^{\parallel} is the same in quadrupole and solenoid

channels. In solenoid channels, there is just one transverse cooling length s_c^\perp . In quadrupole channels, there are two transverse cooling lengths s_x^{-1} and s_y^{-1} .

$$(s_c^\parallel)^{-1} = \frac{1}{pv} \left\langle D_y \frac{\partial}{\partial y} \left(\frac{dE}{ds} \right) + \frac{\partial}{\partial \delta} \left(\frac{dE}{ds} \right) \right\rangle \quad (2)$$

$$(s_c^\perp)^{-1} = \frac{1}{pv} \left\langle \frac{dE}{ds} - \frac{D_y}{2} \frac{\partial}{\partial y} \left(\frac{dE}{ds} \right) \right\rangle \quad (3)$$

$$s_x^{-1} = \frac{1}{pv} \left\langle \frac{dE}{ds} \right\rangle \quad s_y^{-1} = \frac{1}{pv} \left\langle \frac{dE}{ds} - D_y \frac{\partial}{\partial y} \left(\frac{dE}{ds} \right) \right\rangle \quad (4)$$

In a transverse cooling length s_c^\perp , a muon would lose approximately all its energy, if the RF system did not compensate it

The equilibrium emittances ε_\perp^{eq} and $\varepsilon_\parallel^{eq}$ are caused by the balance of cooling and heating by multiple scattering and straggling. The term $13.6\text{MeV}/pv$ is related to multiple scattering. The rate of change per unit length of the RMS relative momentum error $\langle \delta^2 \rangle$ is related to straggling. In (5) and (6), the total muon energy is E , the absorber has radiation length X_0 , dispersion invariant H , and transverse and longitudinal functions β_\perp and β_\parallel . The factor 2 in $D_y/2$ in (5) applies to solenoids.

$$\varepsilon_\perp^{eq} = \frac{E\beta^3\gamma}{2} \left\langle \frac{\overbrace{\beta_\perp \left(\frac{13.6\text{MeV}}{pv} \right)^2 \frac{1}{X_0} + \overbrace{H\langle \delta^2 \rangle}^{\text{straggle}}}{\underbrace{\frac{dE}{ds} - \frac{D_y}{2} \frac{\partial}{\partial y} \left(\frac{dE}{ds} \right)}_{\text{wedge}}}}{\underbrace{\frac{dE}{ds}}_{\text{ionize}}} \right\rangle \quad (5)$$

$$\varepsilon_\parallel^{eq} = \frac{E\beta^3\gamma}{2} \left\langle \frac{\overbrace{\beta_\parallel \langle \delta^2 \rangle}^{\text{straggle}} + \overbrace{\gamma_\parallel D_y^2 \left(\frac{13.6\text{MeV}}{pv} \right)^2 \frac{1}{X_0}}^{\text{scatter}}}{\underbrace{D_y \frac{\partial}{\partial y} \left(\frac{dE}{ds} \right)}_{\text{wedge}} + \underbrace{\frac{\partial}{\partial \delta} \left(\frac{dE}{ds} \right)}_{\text{ionise}}} \right\rangle \quad (6)$$

Partition numbers simplify the notation for cooling lengths and equilibrium emittances in analogy to synchrotron radiation damping. As was the case for the cooling lengths, the longitudinal partition number g_\parallel with $\frac{\partial}{\partial \delta} \left(\frac{dE}{ds} \right) / \frac{dE}{ds} \approx -0.3$ for 200 MeV/c muons in liquid H_2 applies to both quadrupole and solenoid channels. In a solenoid channel there is one transverse partition number g_\perp , while there are two of them, g_x and g_y , in a quadrupole channel.

$$g_{\parallel} = \left\langle D_y \frac{\partial}{\partial y} \left(\frac{dE}{ds} \right) / \frac{dE}{ds} + \frac{\partial}{\partial \delta} \left(\frac{dE}{ds} \right) / \frac{dE}{ds} \right\rangle \quad (7)$$

$$g_{\perp} = \left\langle 1 - \frac{D_y}{2} \frac{\partial}{\partial y} \left(\frac{dE}{ds} \right) / \frac{dE}{ds} \right\rangle \quad (8)$$

$$g_x = 1 \quad g_y = \left\langle 1 - D_y \frac{\partial}{\partial y} \left(\frac{dE}{ds} \right) / \frac{dE}{ds} \right\rangle \quad (9)$$

The partition numbers obey the following sum rule:

$$2g_{\perp} + g_{\parallel} = g_x + g_y + g_{\parallel} = 2 + \frac{\partial}{\partial \delta} \left(\frac{dE}{ds} \right) / \frac{dE}{ds} \quad (10)$$

The absolute value of $|D_y|$ at the absorbers has a lower limit due to the wedge parameter, since it would be nice that the absorber length were positive in the whole vertical aperture. Assuming that the vertical aperture radius is equal to 3 RMS beam radii σ_y , and that the initial relative RMS momentum spread is σ_e^i , one find the following condition:

$$|D_y| \geq 3(1 - g_v)\sigma_y = 3(1 - g_v)\sqrt{\varepsilon_{\perp}^i \beta_{\perp} / (\beta\gamma) + (D_y \sigma_e^i)^2} \quad (11)$$

Solving for $|D_y|$ yields:

$$|D_y| \geq 3(1 - g_v)\sqrt{\frac{\varepsilon_{\perp}^i \beta_{\perp}}{\beta\gamma[1 - (3(1 - g_v)\sigma_e^i)^2]}} \quad (12)$$

Here $|D_y|$ is real and positive if $3(1 - g_v)\sigma_e^i \leq 1$. This is a condition on σ_e^i , which is also found by assuming that σ_y is dominated by σ_e^i , and neglecting the contribution of the betatron oscillations.

Upper limits for $|D_y|$ are due to the cross-plane heating terms in (5) and (6), i.e. the contribution of straggling to ε_{\perp}^{eq} , and of multiple scattering to $\varepsilon_{\parallel}^{eq}$. Assuming that the absorber is at a waist with $\alpha_{\perp} = 0$ and $D'_y = 0$, and using $H = D_y^2 / \beta_{\perp}$, one finds that ε_{\perp} heating due to straggling and $\varepsilon_{\parallel}^{eq}$ heating due to multiple scattering are less than or equal to the heating due to multiple scattering and straggling, if

$$|D_y| \leq \frac{\beta_{\perp}(13.6\text{MeV}/pv)}{\sqrt{X_0\langle\delta^2\rangle}} \quad \text{and} \quad |D_y| \leq \frac{\beta_{\parallel}\sqrt{X_0\langle\delta^2\rangle}}{(13.6\text{MeV}/pv)} \quad (13)$$

The limit on the right hand side of (13) is usually much larger. When D_y is one half of the limit, the cross-plane heating term contributes one quarter of in-plane heating term to the equilibrium emittances.

The linear longitudinal map M , operating on column vector $(ct, \delta p/p)^T$, for arc with slip factor η ; followed by an RF station with RF frequency f_{RF} , harmonic number h , stable phase angle φ_s with origin at the last zero crossing of RF voltage V is:

$$M = \begin{pmatrix} 1 & \frac{ch\eta}{f_{\text{RF}}\beta} \\ \frac{2\pi f_{\text{RF}}eV \cos \varphi_s}{Ec\beta} & 1 + \frac{2\pi\eta h eV \cos \varphi_s}{E\beta^2} \end{pmatrix} \quad (14)$$

From (14), one finds to lowest order in the synchrotron tune Q_{\parallel} :

$$\beta_{\parallel} = \frac{c}{f_{\text{RF}}} \sqrt{-\frac{\eta h E}{2\pi e V \cos \varphi_s}} = \sqrt{-\frac{c\eta C E}{2\pi\beta f_{\text{RF}} e V \cos \varphi_s}} \quad (15)$$

As β_{\perp} , β_{\parallel} has the dimension of length, and the same relations between emittances, beam radii and divergence, and agrees with the definition in MAD [6].

3 RF System and Longitudinal Dynamics

The RF system in a cooling channel must compensate the energy loss in the absorbers and satisfy three conditions: (i) β_{\parallel} must have the value needed to achieve $\varepsilon_{\parallel}^{eq}$ (ii) The bucket height must satisfy $b_{\text{RF}} \approx 2\sigma_e^i$ (iii) The bucket area A_{RF} must match $\varepsilon_{\parallel}^i$. The variables to satisfy these conditions are the slip factor η and the RF frequency f_{RF} . The three limits are discussed below in terms of the the functions $\eta_1(f_{\text{RF}})$, $\eta_2(f_{\text{RF}})$, and $\eta_3(f_{\text{RF}})$. I recall that the average rate of acceleration in the RF cavities is equal to the average rate of energy loss $\langle dE/ds \rangle$, if the muon energies at entrance and exit of the cooling channel are equal. The peak gradient in the RF cavities is obtained by dividing the average gradient by the fraction of the channel occupied by RF cavities < 1 , $\sin \varphi_s < 1$ with stable phase angle φ_s , and the transit time factor < 1 .

Reaching the design value of β_{\parallel} and the bucket height $b_{\text{RF}} = 2\sigma_e^i$ require that η_1 and η_2 , respectively, satisfy:

$$|\eta_1| \leq \frac{2\pi\beta\beta_{\parallel}^2 f_{\text{RF}} \langle dE/ds \rangle}{cE \tan \varphi_s} \quad |\eta_2| = \frac{Y^2(\varphi_s)}{\sin \varphi_s} \frac{c \langle dE/ds \rangle}{4\pi\beta(\sigma_e^i)^2 E f_{\text{RF}}} \quad (16)$$

I avoid fixing the sign of η and the quadrant of φ_s by taking absolute values where needed. The function $Y(\varphi) = \sqrt{|(\pi - 2\varphi) \sin \varphi - 2 \cos \varphi|}$ with $Y(0) = \sqrt{2}$ describes the dependence of b_{RF} on φ . Fig. 1 shows the upper limits for η_1 and η_2 .

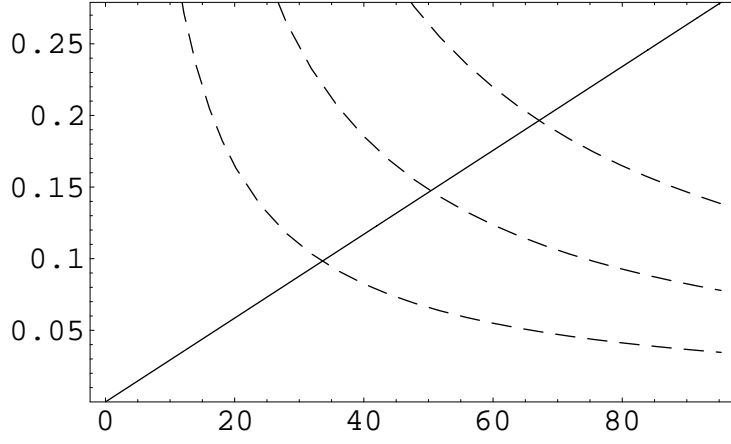


Fig. 1. Upper limits for $|\eta_1|$ and $|\eta_2|$ as functions of f_{RF} in MHz at $\varphi_s = 2\pi/3$. The straight red curve shows the limit $|\eta_1|$ due to β_{\parallel} . The yellow, green and blue hyperbolic curves from above show the limits $|\eta_2|$ for $\sigma_e^i = 0.075, 0.1, 0.15$.

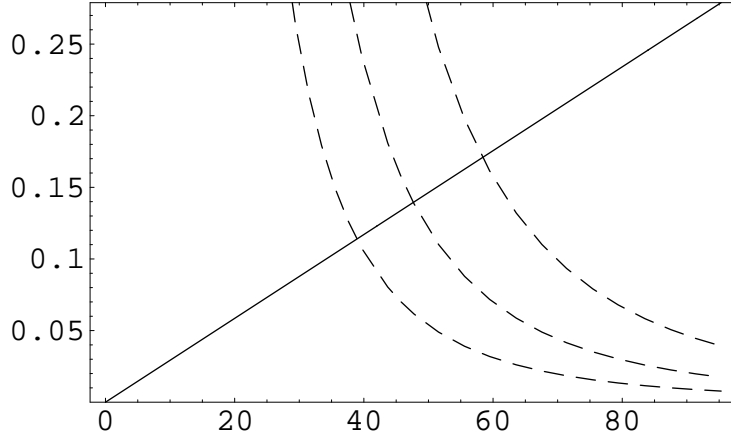


Fig. 2. Upper limits for $|\eta_1|$ and $|\eta_3|$ as functions of f_{RF} in MHz at $\varphi_s = 2\pi/3$. The straight red curve shows the limit $|\eta_1|$ due to β_{\parallel} . The yellow, green and blue hyperbolic curves from above show the limits $|\eta_3|$ for $A_{\text{RF}} = 0.6\pi, 0.9\pi$ and 1.35π m.

Achieving a bucket area $A_{\text{RF}} > 4\pi\varepsilon_{\parallel}^i$ requires

$$|\eta_3| \leq \frac{2\alpha^2(\varphi_s - \pi/2)\langle dE/ds \rangle \gamma}{(\pi\varepsilon_{\parallel}^i)^2 E_{\mu} f_{\text{RF}}^3 \sin \varphi_s} \left(\frac{\beta c}{\pi} \right)^3 \quad (17)$$

Dôme [7] gives a power series for the bucket area function $\alpha(\psi)$ with $\alpha(0) = 0$, $\alpha(\pi/2) = 1$ and ψ counted from the crest. Fig. 3 shows the limits η_1 and η_3 for several values of the stable phase angle φ_s .

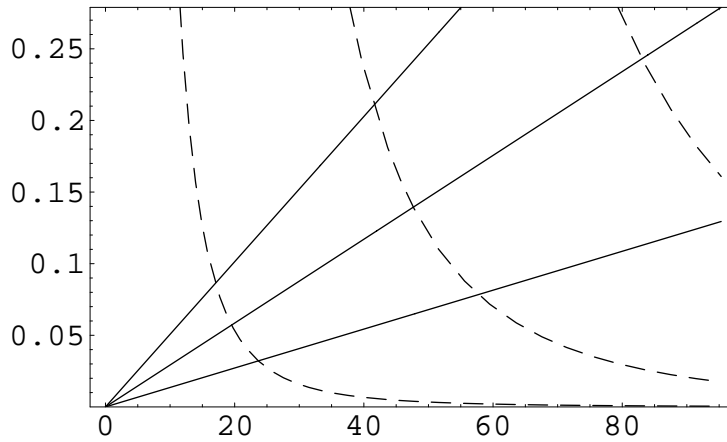


Fig. 3. Upper limits for $|\eta|$ as function of f_{RF} in MHz for $\varphi_s = 5\pi/6, 3\pi/4, 2\pi/3$ from above. The straight curves show the limits $|\eta_1|$ due to β_{\parallel} . The hyperbolic curves show the limits $|\eta_3|$ due to $A_{\text{RF}} = 1.35\pi$ m.

4 Cooling Channel Design

In this Chapter, the formulae in Sections 2 and 3 are used to derive parameters of the cooling channel that is used as an example. They are shown in Tab. 2.

In the first step, the equilibrium emittances and cooling lengths are obtained. From (1) follows that cooling is efficient when $\varepsilon^f \gg \varepsilon^{eq}$. I assume $\varepsilon^{eq} \approx \varepsilon(S)/3 = \varepsilon^f/3$, and solve (1) for s_c . From s_c^{\parallel} and either s_c^{\perp} for a solenoid channel or s_c^y for a quadrupole channel follow the partition numbers g_{\parallel} and either g_{\perp} or g_y as well as the mean rates of energy loss $\langle dE/ds \rangle$ and of acceleration.

In the second step, the transverse amplitude function β_{\perp} is obtained, neglecting the transverse heating due to straggling, i.e. the term proportional to H in (5), and solving it for β_{\perp} with muon rest energy E_{μ} :

$$\beta_{\perp} \leq \frac{2\beta g_{\perp} E_{\mu} X_0 \varepsilon_{\perp}^{eq}}{(13.6\text{MeV})^2} \left(\frac{dE}{ds} \right) \quad (18)$$

Liquid H_2 is the favoured absorber material, because of its large $X_0 dE/ds = 275$ MeV. The absorber length is taken as $L_A = 2\beta_{\perp}$ to limit the variation of β_{\perp} along the absorber. The spacing between absorbers is given by $L_p = L_A dE/ds / \langle dE/ds \rangle$, where $dE/ds = 31.75$ MeV/m is a property of liquid H_2 .

In the third step the longitudinal amplitude function β_{\parallel} is derived, neglecting the longitudinal heating due to scattering, i.e. the term proportional to $1/X_0$ in (6), and finding with the mean square energy variation due to straggling $d\langle \Delta E^2 \rangle / ds = 3.3$ MeV²/m for liquid H_2 noting that the fraction in the large

Table 2

Design parameters of a muon cooling channel. The first block shows the input parameters. The remaining blocks show the computed parameters.

Channel length S	200	m
Muon momentum p	200	MeV/c
Initial normalized emittances $\varepsilon_{\perp}^i/\varepsilon_{\parallel}^i$	10/50	mm
Final normalized emittances $\varepsilon_{\perp}^f/\varepsilon_{\parallel}^f$	$\leq 3/15$	mm
Normalized equilibrium emittance $\varepsilon_{\perp}^{eq}/\varepsilon_{\parallel}^{eq}$	$\leq 1/5$	mm
Cooling length s_c^y/s_c^{\parallel}	133/133	m
Mean rate of energy loss $\langle dE/ds \rangle$	3.8	MeV/m
Amplitude functions at absorber $\beta_{\perp}/\beta_{\parallel}$	0.098/4.05	m
Length of liquid H ₂ absorber L_A	196	mm
Spacing between absorbers L_p	1.65	m
Minimum vertical dispersion $ D_y $	44	mm
Maximum vertical dispersion $ D_y $ from $\varepsilon_{\perp}/\varepsilon_{\parallel}$	0.28/1.41	m
Initial RMS beam radii σ_x/σ_y	22.7/25.4	mm
Initial RMS divergence $\sigma_{x'} = \sigma_{y'}$	232	mr
Initial relative RMS momentum spread σ_e^i	8.1	%
Initial RMS bunch length σ_s	289	mm
Stable phase angle φ_s	$2\pi/3$	
Frequency f_{RF}	47.7	MHz
Maximum slip factor η	0.139	

brackets depends only on the absorber material:

$$\beta_{\parallel} \leq \frac{2E_{\mu} g_{\parallel} \varepsilon_{\parallel}^{eq}}{\beta} \left(\frac{\frac{dE}{ds}}{\frac{d(\Delta E^2)}{ds}} \right) \quad (19)$$

In the fourth step, the muon beam parameters at the absorber are obtained. The initial RMS beam radii σ_x and σ_y , and both divergences σ' at the centre of absorber follow from the initial transverse emittance ε_{\perp}^i , initial relative RMS energy spread σ_e^i , β_{\perp} and D_y , assuming $D'_x = D'_y = 0$:

$$\sigma_x = \sqrt{\varepsilon_{\perp}^i \beta_{\perp} / \beta \gamma}; \quad \sigma_y = \sqrt{\varepsilon_{\perp}^i \beta_{\perp} / \beta \gamma + (D_y \sigma_e^i)^2}; \quad \sigma' = \sqrt{\varepsilon_{\perp}^i / \beta \gamma \beta_{\perp}} \quad (20)$$

In Tab. 2 I assume that $|D_y|$ has half of the smaller value in (13). The bunches

are longitudinally matched to the buckets, i.e. bunch length σ_s and σ_e^i follow from $\varepsilon_{\parallel}^i$ and β_{\parallel} .

In the fifth step, the slip factor $|\eta|$ and the RF frequency f_{RF} are calculated. The maximum value of $|\eta|$ as a function of f_{RF} is given by η_1 at low f_{RF} , by η_3 at high f_{RF} , and by η_2 at intermediate f_{RF} , although $\eta_2(f_{\text{RF}})$ may be higher than $\eta_3(f_{\text{RF}})$. I determine η and f_{RF} by finding the frequencies f_{ik} with $\eta_i = \eta_k$ for $i, k = 1, 2, 3$, using the larger of f_{13} and f_{23} as f_{RF} , and obtaining the maximum value from $\eta = \eta_3(f_{\text{RF}})$. By this choice of f_{RF} , $|\eta|$ drops like f^{-3} above f_{RF} . Tab. 2 shows the results for $|\eta|$ and f_{RF} .

Table 3

Comparison between the transverse parameters of quadrupole and solenoid cooling channels. The input parameters are the same for both styles, and listed in Tab. 2

	Quad	Sol	
Transv. part. nos. g_h/g_v	1/0.353	0.568/0.568	
Transv. amplitude fct. β_{\perp}	78	126	mm
Length of absorber L_A	157	253	mm
Wedge param. $D_y L_A / L'_A$	0.647	0.432	
Absorber spacing L_p	1.32	3.43	m
Minimum $ D_y $	40	33	mm
Maximum $ D_y $ from $\varepsilon_{\perp} / \varepsilon_{\parallel}$	0.23/1.4	0.36/2.3	m
Initial RMS radii σ_x / σ_y	20.3/22.3	25.8/28.3	mm
Initial RMS divergence σ'	260	205	mr

5 Second Round of Cooling Channel Design

In this second round of the cooling ring design, the heating due to straggling is assumed to contribute 25 % to ε_{\perp}^{eq} , by operating the cooling channel at a value of D_y that is one half of the smaller limit in Tab. 2. The heating of $\varepsilon_{\parallel}^{eq}$ due to multiple scattering is still ignored. This assumption is justified, since the limit on D_y is an order of magnitude larger.

I also compare a quadrupole and a solenoid cooling channel with identical input parameters. The quadrupole channel damps faster in the horizontal plane than in the vertical plane where the length of the absorbers varies. The horizontal final and equilibrium emittances are smaller than the vertical ones. This is the reason for the \leq signs in Tab. 2. A solenoid channel damps equally in the horizontal and vertical direction. The final and equilibrium emittances are equal in both directions. Tab. 3 and 4 show the results for the transverse

and longitudinal parameters, respectively. Also shown are the merit factors M , i.e. the ratios of final over initial phase space density with muon lifetime τ_μ , excluding other muon losses that are outside the scope of the analytical theory.

$$M = \frac{\varepsilon_x^i \varepsilon_y^i \varepsilon_\parallel^i}{\varepsilon_x^f \varepsilon_y^f \varepsilon_\parallel^f} \exp\left(-\frac{S}{\beta\gamma c\tau_\mu}\right) \quad (21)$$

A quadrupole channel is harder than a solenoid channel, but promises better performance.

Table 4

Comparison between the longitudinal parameters of quadrupole and solenoid cooling channels. The input parameters are the same for both styles, and listed in Tab. 2

	Quad	Sol	
Long. part. no. g_\parallel	0.353	0.568	
Mean energy loss rate $\langle dE/ds \rangle$	3.77	2.34	MeV/m
Long. amplitude function β_\parallel	4.05	6.5	m
RMS bunch length σ_s	0.29	0.37	m
RMS rel. momentum spread σ_e	8.1	6.4	%
Stable phase angle φ_s	$2\pi/3$	$2\pi/3$	
Frequency f_{RF}	47.7	37.5	MHz
Maximum slip factor η	0.139	0.177	
Merit factor M	194	31.5	

6 Conclusions

A design procedure is presented for muon cooling channels that are either straight or ring-shaped, with focusing either by quadrupoles or by solenoids. It is based on analytical theory which needs only nine channel parameters p , ε_x^i , ε_y^i , ε_\parallel^i , ε_\perp^f , ε_\parallel^f , ε_\perp^{eq} , $\varepsilon_\parallel^{eq}$, S , and three absorber parameters X_0 , dE/ds , $d\langle\Delta E^2\rangle/ds$, and is suitable for search of parameters that warrant detailed studies by simulation. The time for calculating a set of parameters is short compared to the time needed for entering the data. The physics incorporated in the design procedure is discussed. However, many engineering details of muon cooling channels are omitted.

References

- [1] N. Holtkamp and D. Finley (eds.), A Feasibility Study of a Neutrino Source Based on a Muon Storage Ring, FERMILAB-PUB-00-108-E (2000)
- [2] S. Ozaki, R. Palmer, M. Zisman and J. Gallardo, (eds.), Feasibility Study II of a Muon-Based Neutrino Source, BNL-52623 (June 2001)
- [3] A. Blondel, The international muon cooling experiment MICE, this workshop.
- [4] D. Neuffer, Overview of Ionisation Cooling, this workshop.
- [5] C-x Wang, Beam-Envelope Theory of Ionisation Cooling, this workshop.
- [6] H. Grote and F.C. Iselin, The MAD Program, Version 8.16, User's Reference Manual, CERN SL/90-13(AP) Rev. 4 (1995).
- [7] G. Dôme, Theory of RF Acceleration, in: CERN 87-03 (1987) 110.